Anal Bioanal Chem (2011) 400:2953–2961
DOI 10.1007/s00216-011-4958-7

ORIGINAL PAPER

Simultaneous profiling of lysophospholipids and phospholipids from human plasma by nanoflow liquid chromatography-tandem mass spectrometry

Ju Yong Lee · Hye Kyeong Min · Myeong Hee Moon

Received: 5 January 2011 / Revised: 11 March 2011 / Accepted: 26 March 2011 / Published online: 18 April 2011

Abstract In this study, an analytical method for the simultaneous separation and characterization of various molecular species of lysophospholipids (LPLs) and phospholipids (PLs) is introduced by employing nanoflow liquid chromatography-electrospray ionization tandem mass spectrometry (nLC-ESI-MS/MS). Since LPLs and PLs in human plasma are potential biomarkers for cancer, development of a sophisticated analytical method for the simultaneous profiling of these molecules is important. Standard species of LPLs and PLs were examined to establish a separation condition using a capillary LC column followed by MS scans and data-dependent collision-induced dissociation (CID) analysis for structural identification. With nLC-ESI-MS/MS, regioisomers of each category of LPLs were completely separated and identified with characteristic CID spectra. It was applied to the comprehensive profiling of LPLs and PLs from a human blood plasma sample and yielded identifications of 50 LPLs (each regioisomer pair of 6 lysophosphatidylcholines (LPCs), 7 lysophosphatidylethanolamines (LPEs), 9 lysophosphatidic acid (LPAs), 2 lysophosphatidylglycerols (LPGs), and 1 lysophosphatidylserine (LPS)) and 62 PLs (19 phosphatidylcholines (PCs), 11 phosphatidylethanolamines (PEs), 3 phosphatidylserines (PSs), 16 phosphatidylinositols (PIs), 8 phosphatidylglycerols (PGs), and 5 phosphatidic acids (PAs)).

Keywords nLC-ESI-MS/MS · Lysophospholipids · Phospholipids · Human plasma · Tandem mass spectrometry

Introduction

Phospholipids (PLs) are major components of cellular membranes and are classified into molecular species based on differences in the polar head group and in the acyl chain length along with the degree of unsaturation. PLs are associated with cell proliferation, apoptosis, and signal transduction [1–3]. While PLs have two acyl chains and a phosphate with characteristic head groups linked to a glycerol backbone, lysophospholipids (LPLs) have one acyl chain in either the sn-1 or sn-2 position of the glycerol backbone. LPLs, mostly produced by the enzymatic reaction of phospholipases, are also involved in signaling mechanisms and in the pathway of disease development [4–6]. In particular, lysophosphatidylcholine (LPC) and lysophosphatidic acid (LPA) in plasma have been reported as clinically important potential biomarkers of human cancers such as ovarian and colorectal cancer, respectively [7–9]. Therefore, qualitative and quantitative analyses of LPLs and PLs are of interest to determine the relationship of diseases and the changes in composition and concentration of lipid species in biological fluid.

Analytical methods that have been in use for lipidomics were well introduced in recent review articles [3, 10]. Analyses of PLs were carried out with gas chromatography-mass spectrometry (MS) after derivatization [11, 12] and thin layer chromatography with matrix-assisted laser desorption and ionization time-of-flight (MALDI-TOF) MS [13, 14] or densitometry [15]. Structural characterization of LPLs and PLs were made with the help of sophisticated electrospray ionization tandem mass spectrometry (ESI-MS/MS) [16–19].

Electronic supplementary material The online version of this article (doi:10.1007/s00216-011-4958-7) contains supplementary material, which is available to authorized users.

J. Y. Lee · H. K. Min · M. H. Moon (✉)
Department of Chemistry, Yonsei University,
Seoul 120-749, South Korea
e-mail: mhmoon@yonsei.ac.kr

In a recent report, LPLs and PLs in rat brain sections after ischemic stroke were simultaneously characterized using MALDI-MS/MS [20]. Coupling liquid chromatography (LC) with ESI-MS/MS allowed separation of intact PLs and simultaneous identification of structures as well [21–24]. Nanoflow LC with ESI-MS/MS (nLC-ESI-MS/MS) has recently been utilized to study PLs from human urine samples of breast cancer [25–27]. Analysis of LPLs was made with ESI-MS for plasma sample of gynecological cancer [28] and ovarian cancer [8]. LC-ESI-MS was utilized to study LPLs from plasma samples [5, 6, 9, 29, 30], bronchoalveolar lavage fluid [4], and soy protein isolate (SPI) [31]. The latter work [31] resulted in the characterization of 56 LPLs in SPI using LC-ESI-MS/MS for the first time, but it took a long time (60–80 min) for separation of entire LPLs by high-performance liquid chromatography (HPLC).

This study introduces a comprehensive separation and characterization method for both LPLs and PLs simultaneously in human blood plasma using nLC-ESI-MS/MS. Separation of LPLs and PLs were first evaluated with various standard species of LPLs and PLs by capillary LC which can improve separation speed, followed by a data-dependent collision-induced dissociation (CID) for the structural determination which was run under both positive and negative ion modes of MS. It demonstrates that with nLC-ESI-MS/MS, regioisomers of each category of LPLs can be completely separated and identified with characteristic CID spectra. Experiments were further applied to a human blood plasma sample for the characterization of regioisomers of five groups of LPLs (lysophosphatidylcholines (LPCs), lysophosphatidylethanolamines (LPEs), lysophosphatidylserines (LPSs), lysophosphatidylglycerols (LPGs), and lysophosphatidic acids (LPAs)) and of six groups of PLs (PCs, PEs, PSs, PGs, PIs, and PAs).

Experimental

Materials and plasma sample

Standard lipids examined were seven LPLs (12:0 LPC, 16:0 LPC, 14:0 LPE, 14:0 LPA, 14:0 LPG, 18:0 LPS, and 18:1 LPI) and nine PLs (12:0/12:0 PE, 12:0/12:0 PC, 14:0/16:0 PC, 20:0/20:0 PC, 12:0/12:0 PA, 12:0/12:0 PS, 14:0/14:0 PS, 16:0/18:1 PI, and 18:0/20:4 PI), which were purchased from Avanti Polar Lipids Inc. (Alabaster, AL, USA). These standards were dissolved in a solution of 60% (*v*/*v*) CH_3OH with 20% (*v*/*v*) $CHCl_3$ in dH_2O, and the dissolved mixture was diluted with CH_3OH/CH_3CN (9:1, *v*/*v*) for the nLC-ESI-MS/MS run. A human plasma sample was obtained from a healthy female volunteer (age 25). For extraction of lipids, 200 μL of the plasma sample was diluted with 500 μL of PBS solution, and then the Folch method [32] was utilized with a slight modification. The diluted mixture was mixed with 2.1 mL of $CH_3OH/CHCl_3$ (2:1) and vortexed for 10 min. After adding 0.4 mL of dH_2O to the mixture followed by vortexing, the mixture solution was centrifuged at 15,000×*g* for 5 min for phase separation. The upper layer, consisting of water, was collected to repeat the above extraction procedure once more. The bottom layer containing lipids was dried with a SpeedVac® Plus (ThermoSavant, Waltham, MA, USA). The measured weight of final extracted lipid mixture was 2.5 mg, and this was re-dissolved in CH_3OH/CH_3CN (1:1) in a final volume of 500 μL; these samples were stored at −20 °C. For nLC-ESI-MS/MS analysis, this mixture was diluted to 5 μg/μL in the mobile phase B (90/10 (*v*/*v*) isopropanol/CH_3CN) for nLC-ESI-MS/MS analysis.

Nanoflow LC-ESI-MS/MS of LPLs and PLs from human plasma

A capillary LC column was prepared from silica capillaries (75 μm I.D., 360 μm O.D., and 17 cm length) obtained from Polymicro Technology, LLC (Phoenix, AZ, USA) by packing Magic C18 (5 μm–100 Å) reverse-phase resin from Michrom Bioresources, Inc. (Auburn, CA, USA). Before packing the column, one end of the capillary was pulled with a flame to construct a sharp self-emitter for ESI and then was packed with a methanol slurry of the resin with He under 1,000 psi. HPLC grade solvents (CH_3CN, CH_3OH, $CHCl_3$, isopropanol, and dH_2O) were used.

For nLC-ESI-MS/MS, a model 1200 binary pump system with an autosampler from Agilent Technologies (Palo Alto, CA, USA) with LCQ Deca XP MAX ion trap mass spectrometer from Thermo Finnigan (San Jose, CA, USA) was used. The pump flow was connected to the pulled-tip capillary column via a PEEK microcross from Upchurch Scientific (Oak Harbor, WA, USA), in which two other ports were used for the connection of a Pt wire for electrical contact and for vent tubing. The vent tubing was controlled by an on–off valve connected at the other end. The vent tubing was closed during sample loading, but was left open during gradient separation so that the pump flow could be split to generate a flow rate of 300 nL/min through the analytical column. Mobile phase solutions for binary gradient elution of LC were 90/10 (*v*/*v*) dH_2O/CH_3CN for A and 90/10 (*v*/*v*) isopropanol/CH_3CN for B. Different modifiers were added to each solution: 0.1% formic acid for the positive ion mode of MS analysis and 0.05% NH_4OH for the negative ion mode. A sample mixture of LPLs and PLs was loaded onto the analytical column at a flow rate of 300 nL/min for 10 min using mobile phase A. The injection amounts of each LPL and PL standard were fixed at 1 pmol for positive ion mode and 0.8 pmol for

negative ion mode. For the plasma extract sample, 15 μg (correspond to 1.2 μL of plasma sample) and 10 μg (0.8 μL) were injected for the positive and negative ion mode of analysis, respectively. After sample loading, a binary gradient was started with a flow rate of 7 μL/min from the pump, while the on–off valve of the vent tubing was open so that a reduced flow rate (300 nL/min) could be delivered to the column, to minimize dwell time. For binary gradient elution, different gradient conditions were used for each ion mode. For the positive ion mode of detection, mobile phase B was ramped from 0% to 40% over 1 min after completing sample loading, linearly increased to 100% over 69 min, and then maintained at 100% for 40 min (gradient-I). For the negative ion mode of detection, two gradient conditions were utilized as follows. In the gradient-II condition, mobile phase B was ramped to 50% over 1 min, linearly increased to 60% over 14 min, to 100% over 10 min, and then maintained for 35 min. In the gradient-III, mobile phase B was increased to 30% over 1 min, to 60% over 39 min, and maintained for 10 min. For ESI, 2.5 and 3.0 kV were applied for the positive and negative ion modes, respectively. At each MS scan, data-dependent CID analysis of the three most intense ions was carried out under 40% (positive ion mode) or 45% (negative) of normalized collision energies. Mass ranges of MS scans were 400–900 amu for the positive ion mode and 350–930 amu for the negative ion mode. During the MS scan in positive ion mode, mass ranges *m/z* 531.6~532.6 were rejected to remove interfering peaks that were thought to be from fluorinated ethylene propylene (FEP) tubing in the pump and silica capillary tubings.

Results and discussion

Analysis of standard LPLs and PLs in the positive ion mode of nLC-ESI-MS/MS

Standard LPLs and PLs with head groups of choline and ethanolamine such as LPC, LPE, PC, and PE were utilized to establish a run condition in the positive ion mode of nLC-ESI-MS/MS. LPLs and PLs containing other head groups such as inositol, serine, glycerol, and hydrogen (phosphatidic acid (PA)) were analyzed in the negative ion mode of nLC-ESI-MS/MS.

Figure 1 shows the base peak chromatogram (BPC) of the mixture of seven LPE, LPC, PE, and PC standards obtained by the positive ion mode of nLC-ESI-MS/MS. We selected these standards to develop an analytical condition to separate LPLs and PLs having a broad range of acyl chain lengths so that numerous LPLs and PLs in real biological samples could be accommodated for separation. The types of acyl chains and the head groups of the seven

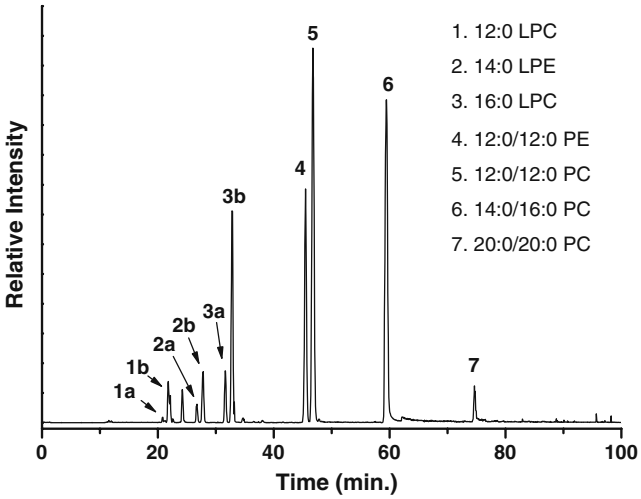

Fig. 1 Base peak chromatogram (BPC) of seven standard phospholipids (LPC, LPE, PC, and PE) at the positive ion mode of nLC-ESI-MS/MS using the gradient-I condition. Identity of each standard molecule is listed inside the figure with the carbon chain length and number of double bonds. The *a* and *b* after each sample number represent the sn-2(acyl/lyso-LPL) and sn-1(lyso/acyl-LPL) regioisomers of LPLs, respectively. Binary gradient LC run conditions are explained in the "Experimental" section

standards are represented inside Fig. 1 by numbers. Since LPLs have only one acyl chain with the other acyl chain replaced by a hydroxyl group in either the sn-1 or sn-2 carbon of the glycerol molecule, they elute earlier than PLs, as shown in Fig. 1, and elute with an increasing number of acyl chain lengths for LPCs and PCs. Each LPL molecule in the current separation is clearly distinguished by the separation of regioisomers, which differs by the position of the acyl chain attached to the glycerol carbon and are represented as a and b in Fig. 1. For standard 12:0-LPC molecules, peaks 1a and 1b represent the regioisomers lyso/12:0-PC and 12:0/lyso-PC, respectively, and usually display a latter peak more abundantly than the first one. This phenomenon is also observed for the other two standards (standards 2 and 3 in Fig. 1). The notation of lyso/12:0-PC represents that the hydroxyl group is attached to the sn-1 carbon of glycerol, and that the acyl chain having 12 carbons without a double bond is attached to the sn-2 carbon (sn-1 lyso subspecies). The molecular structures of these regioisomers can be determined from the data-dependent CID experiment during the nLC-ESI-MS/MS run. Figure 2 shows the CID spectra of parent ions (a) 1a, (b) 1b, (c) 3a, (d) 3b, (e) 2a, and (f) 2b. MS/MS spectra of the parent ion 1a (*m/z*440.5) yielded the two major peaks that are the prominent fragment ion at *m/z*184.3 from the phosphocholine cation ($H_2PO_4(CH_2)_2N(CH_3)_3$, 184 amu), which is an important indicator of the presence of a choline head group and the ion at *m/z*422.8 from $[M+H\text{-}H_2O]^+$. Minor peaks shown in the inset of Fig. 2a represent the fragment ions of *m/z*240.9 and 259.1 from the loss of a

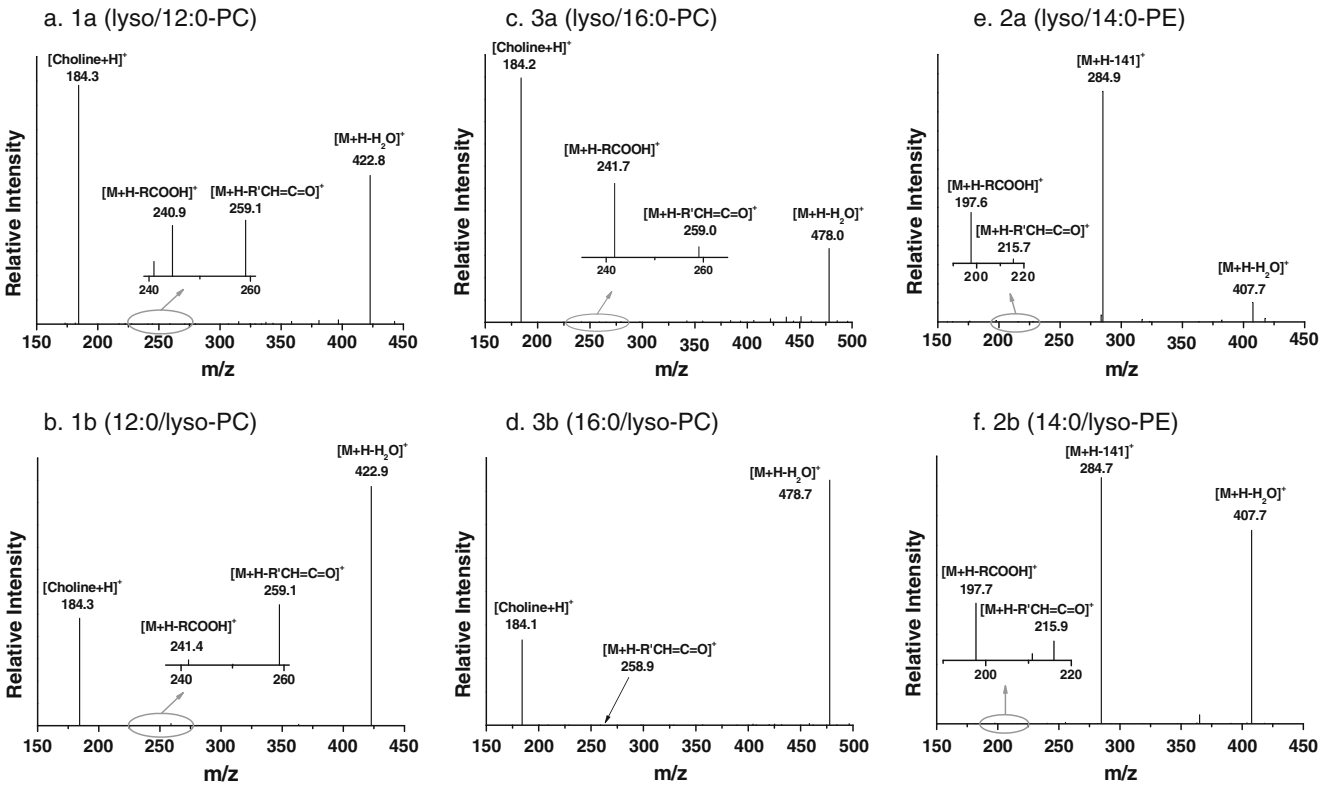

Fig. 2 Data-dependent CID spectra of peaks **a** 1a, **b** 1b, **c** 3a, **d** 3b, **e** 2a, and **f** 2b regioisomers shown in Fig. 1

fatty acid (at sn-1) in the form of carboxylic acid ($[M+H-RCOOH]^+$) and ketene ($[M+H-R'CH=C=O]^+$), respectively. CID spectra of the parent ion 1b in Fig. 2b show similar fragment ions except for the difference in the relative ratio of intensities of the phosphocholine cation and $[M+H-H_2O]^+$, in which the intensity of the latter is relatively large for the 12:0/lyso-PC (sn-2 lyso-PC) compared to lyso/12:0-PC (sn-1 lyso-PC). In Fig. 2c, d, CID spectra of another LPC regioisomers (16:0-LPC: 3a and 3b shown in Fig. 1) show the similar fragmentation patterns observed in Fig. 2a, b. Same fragment ions of *m/z* 241.7 and 259.0 appear from fragmentation of lyso/16:0-PC as observed with the same ions in Fig. 1a, demonstrating that loss of a fatty acid in the form of carboxylic acid, and ketene is confirmed. In

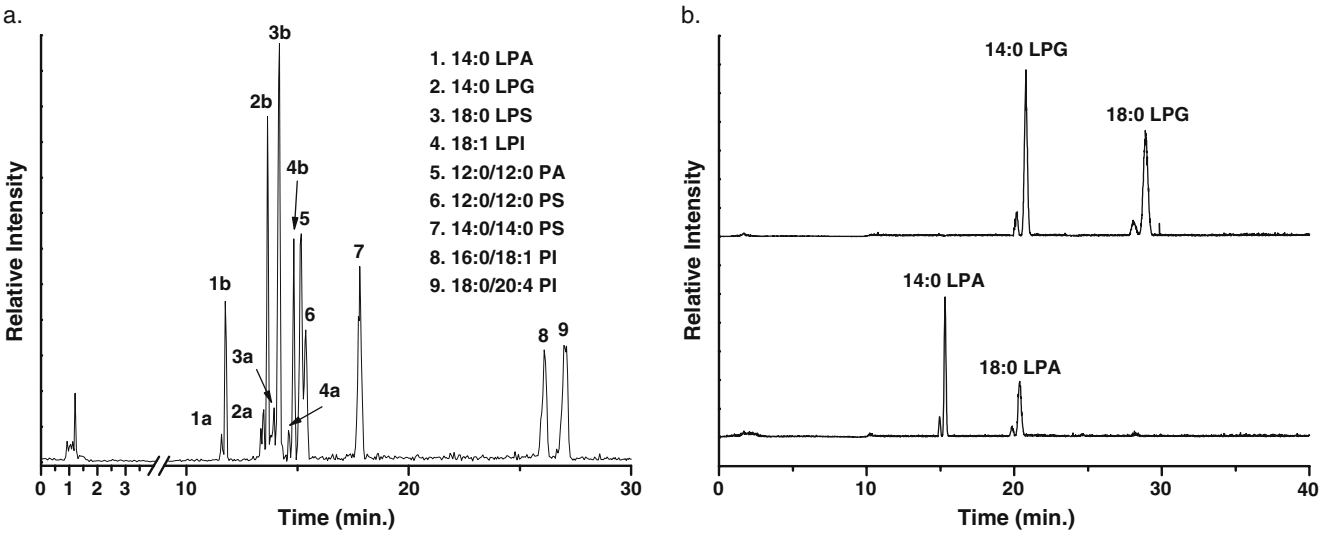

Fig. 3 **a** BPC of nine standard phospholipids (LPA, LPG, LPS, LPI, PA, PS, and PI) at negative ion mode of nLC-ESI-MS/MS (gradient-II) and **b** BPCs of LPGs and LPAs (gradient-III). The *a* and *b* after each sample number represent the sn-2 (acyl/lyso-LPL) and sn-1(lyso/acyl-LPL) regioisomers of LPLs, respectively

addition, the relative ratio of the phosphocholine cation (*m/z* 184.1 at Fig. 2d) and the water-dissociated parent ion (*m/z* 478.7) shows the same tendency with the stronger intensity of the latter peak for the sn-2 lyso-PC. This difference in ion intensities, along with different retention time in nLC, can be an indicator to distinguish regioisomers of LPC. It is noted that lyso/12:0-PC elutes earlier than 12:0/lyso-PC, since hydrophobic interaction between the acyl chain and the C18 stationary phase becomes stronger when the acyl chain is attached at the sn-1 carbon of the glycerol backbone rather than at sn-2. This is because the acyl chain that is attached to the sn-1 carbon of LPC becomes more extended in molecular geometry. For the case of 14:0-LPE (*m/z*426.3) in Fig. 2e, f, base peak fragment ions are observed at *m/z*284.9 from $[M+H-141]^+$, which is the loss of phosphoethanolamine ($HPO_4(CH_2)_2NH_3$, 141 amu), and at *m/z*407.7 from $[M+H-H_2O]^+$. The characteristic ion from the phosphoethanolamine cation (*m/z*141 amu) in LPE is not observed for the identification of LPE. However, identification of LPE regioisomers can be made with the difference of retention times and the relative intensity of the two major fragment ion peaks: $[M+H-141]^+$ and $[M+H-H_2O]^+$. For PE and PCs, it is rather straightforward to identify the structure of the molecules from CID spectra when the two acyl chains are different from each other. In our earlier studies [22, 23, 26], identification of PC and PE molecules from nLC-ESI-MS/MS are clearly described, and thus, it is not necessary to go over in this report. However, identification of the PC regioisomers is straightforward since the formation of the $[M+H-R_2'CH=C=O]^+$ ion over ($[M+H-R_1'CH=C=O]^+$ is preferred in the CID of PC as reported in references [16, 22]. An example of CID spectra of PC regioisomers (14:0/16:0-PC and 16:0/14:0-PC) is included in the Electronic Supplementary Material Figure S1.

Limit of detection (LOD) values of LPC and LPE for the current nLC-ESI-MS/MS method were calculated within the concentration range of 10 fmol~2 pmol of few standard LPLs and PLs, and the calculated LODs were 2.0 fmol (*S* (calibration sensitivity)=0.57, r^2=0.990) for 12:0-LPC, 2.6 fmol (*S*=0.63, r^2=0.999) for14:0-LPE, and 1.2 fmol (*S*=2.00, r^2=0.987) for 12:0/12:0-PC at a signal-to-noise ratio of 3.

Analysis of standard LPLs and PLs in negative ion mode of nLC-ESI-MS/MS

In the negative ion mode of nLC-ESI-MS/MS, LPLs and PLs containing one of four polar head groups such as inositol, serine, glycerol, and hydrogen attached to phosphate can be identified with separation of the regioisomers of LPLs as observed similar to those in Fig. 1. Figure 3a

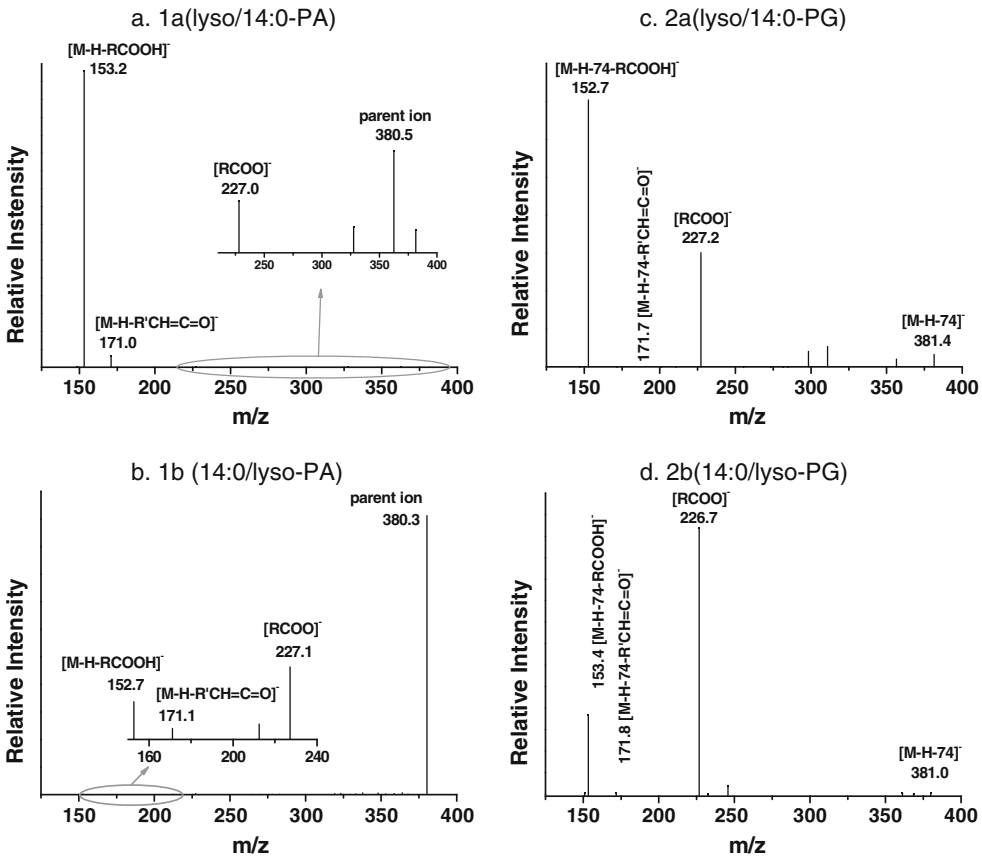

Fig. 4 Data-dependent CID spectra of regioisomers of 14:0-LPA (peaks 1a, 1b) and 14:0-LPG (peaks 2a, 2b) shown in Fig. 3. CID spectra of each regioisomer are compared

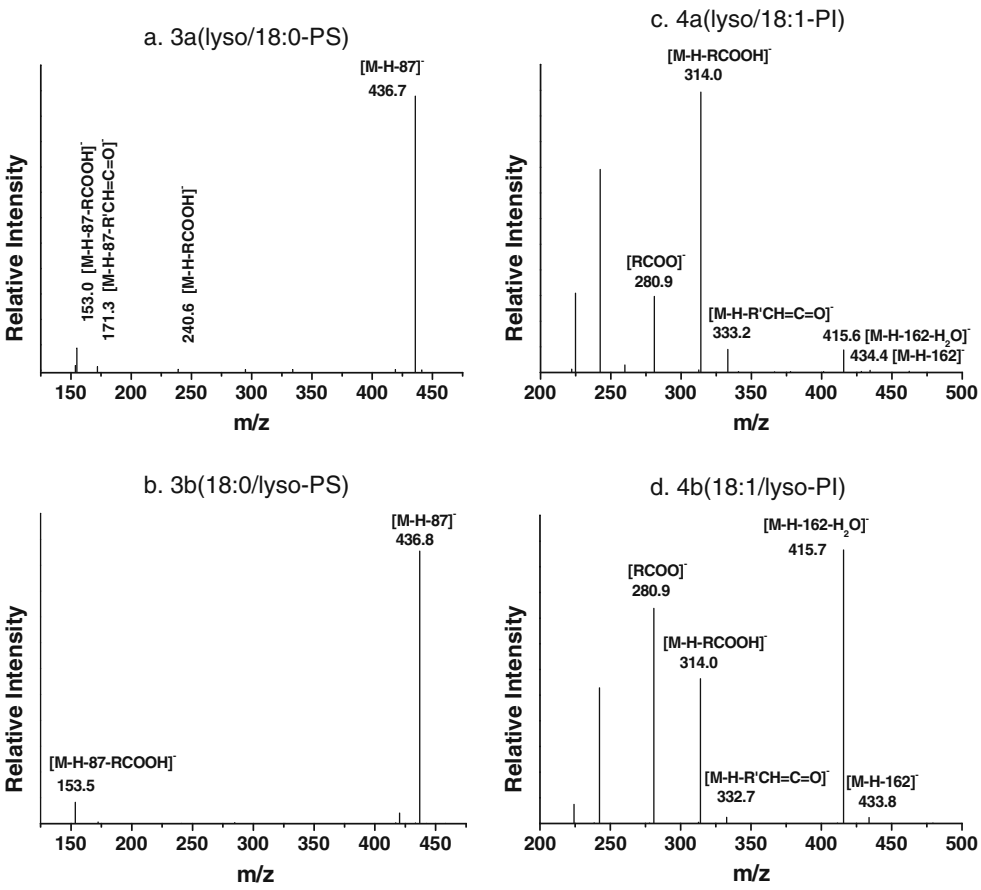

Fig. 5 CID spectra of regioisomers of 18:0-LPS (peaks 3a, 3b) and 18:1-LPI (peaks 4a, 4b) shown in Fig. 3

shows the separation of four LPLs and five PL standards at a gradient run condition II (see "Experimental" section). Regioisomers of each LPL are marked as a and b, representing the isomers as described above. Upon the separation order, it is shown that regioisomers of LPLs with sn-1 lyso-PLs (or lyso/acyl-PLs) eluted earlier than sn-2 lyso-PLs as similarly observed for LPC and LPE in Fig. 1. Figure 3b shows improved separations of two LPG standards (top chromatogram) and of two LPAs (bottom) obtained at a different gradient elution condition (see the gradient-III in "Experimental" section), which provides a clear separation of regioisomers. Molecular structures of regioisomers are determined by CID spectra of each species similar to those in Fig. 2. CID spectra of molecular ions 1a

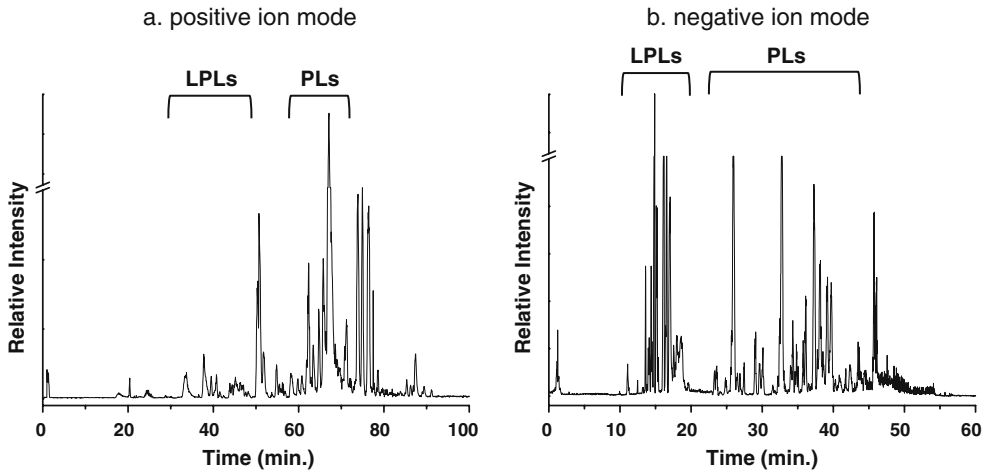

Fig. 6 Base peak chromatogram of a human blood plasma extract by **a** positive and **b** negative ion modes of nLC-ESI-MS/MS. LC run conditions used for positive and negative ion modes are the same as used for Figs. 1 and 3, respectively

Table 1 Identified LPLs and PLs from (a) positive ion mode and (b) negative ion mode of nLC-ESI-MS/MS for human plasma sample

Class	Molecular species	t_r	m/z
Positive ion mode			
LPC	lyso/18:2	31.9	520.6
	lyso/18:1	32.0	522.6
	lyso/20:4	32.1	544.7
	lyso/22:6	32.2	568.6
	18:2/lyso	33.2	520.6
	18:1/lyso	33.4	522.6
	20:4//lyso	33.4	544.7
	lyso/16:0	33.8	496.5
	lyso/18:0	34.3	524.5
	16:0/lyso	34.3	496.5
	18:0/lyso	34.8	524.5
	22:6/lyso	36.3	568.6
LPE	lyso/18:2	33.1	478.5
	lyso/18:1	33.1	480.5
	lyso/20:3	33.2	504.7
	lyso/20:4	33.7	502.5
	18:2/lyso	33.8	478.5
	18:1/lyso	33.9	480.5
	20:3/lyso	34.3	504.7
	20:4//lyso	34.7	502.5
	lyso/18:0	40.8	482.5
	lyso/16:0	41.2	455.3
	18:0/lyso	41.8	482.5
	16:0/lyso	41.9	455.3
	lyso/22:6	45.0	526.6
	22:6/lyso	47.0	526.6
PC	16:0/20:5	59.4	780.8
	16:0/20:4	59.5	782.6
	18:3/20:3	59.5	806.5
	16:0/16:0	60.0	735.4
	16:0/18:2	60.7	758.7
	18:2/20:4	61.3	806.8
	16:0/18:1	61.8	761.4
	16:1/22:6	61.9	804.5
	20:1/18:4	62.2	808.9
	18:1/18:1	62.3	786.7
	16:1/20:2	62.4	784.5
	18:2/18:1	62.5	784.7
	18:0/20:4	63.8	810.5
	16:3/18:5	64.2	746.7
	18:0/18:2	65.2	786.8
	18:1/18:0	65.7	788.7
	16:0/20:2	65.8	786.8
	18:1/22:6	65.9	833.1
	20:3/18:0	66.9	812.7
PE	20:4/18:2	62.4	764.8
	18:1/22:6	63.2	790.5
	18:1/20:4	63.7	766.7
	22:2/14:1	63.7	742.9
	20:1/20:4	64.7	794.6
	16:0/20:1	66.6	746.7
	20:0/16:1	66.7	746.9
	22:1/18:3	67.1	797.3
	20:1/20:3	68.2	796.9
	16:0/20:3	71.6	743.1
	22:0/18:4	71.9	796.8
Negative ion mode			
LPA	lyso/14:0	12.9	380.9
	14:0/lyso	13.7	380.9
	lyso/16:0	14.3	408.7
	lyso/18:2	15.3	433.1
	16:0/lyso	15.3	408.7
	lyso/18:3	15.3	431.1
	lyso/16:2	15.7	405.2
	18:2/lyso	16.1	431.1
	lyso/18:0	16.2	437.1
	18:3/lyso	16.2	433.1
	lyso/20:4	16.3	456.8
	16:2/lyso	16.5	405.2
	lyso/16:1	16.8	407.4
	20:4/lyso	16.9	456.8
	lyso/22:6	17.5	481.2
	16:1/lyso	17.6	407.4
	18:0/lyso	17.8	437.1
	22:6/lyso	18.4	481.2
LPG	lyso/16:0	13.8	482.9
	lyso/18:0	17.1	510.7
	16:0/lyso	14.5	482.9
	18:0/lyso	18.0	510.7
LPS	lyso/18:0	14.1	524.2
	18:0/lyso	15.0	524.2
PS	18:0/18:0	24.0	790.7
	18:0/18:1	24.4	789.1
	18:1/20:0	26.4	817.2
PI	16:0/20:4	23.6	857.9
	18:1/16:0	25.3	835.5
	16:0/18:2	25.3	834.1
	16:0/22:6	25.5	881.7
	16:0/20:3	25.6	859.6
	18:1/20:4	26.0	883.8
	16:0/18:1	26.7	836.2
	18:0/18:2	27.4	862.2
	18:1/18:1	27.4	861.4
	18:0/22:6	27.5	909.6
	18:0/20:4	27.6	885.8
	18:0/22:5	27.9	911.7

Table 1 (continued)

Class	Molecular species	t_r	*m/z*
	18:0/20:2	28.1	889.9
	18:0/20:3	28.1	887.9
	18:0/18:1	28.5	864.1
	20:2/20:1	34.2	915.8
PG	18:2/20:0	28.1	801.1
	18:0/14:3	32.6	715.8
	18:2/18:0	32.8	774.2
	20:4/18:0	34.0	798.4
	16:2/20:4	37.2	767.7
	20:0/16:3	37.9	771.1
	22:6/18:0	39.2	821.7
	18:2/20:5	43.4	730.9
PA	16:1/22:6	32.6	717.3
	18:2/22:6	32.6	742.8
	18:2/20:0	32.6	727.6
	20:4/20:0	32.8	751.2
	20:4/22:6	33.7	767.1

(lyso/14:0-PA, *m/z*381.2), in Fig. 4a, show the base peak at *m/z*153.2 and an ion peak at *m/z*171.0 that are formed from the dissociation of the acyl chain as it forms $[M\text{-}H\text{-}RCOOH]^-$ and $[M\text{-}H\text{-}R'CH{=}C{=}O]^-$, respectively. Enlarged spectra, inset, show the parent ion peak $[M\text{-}H]^-$ at *m/z*380.5 along with carboxylate anion peak $[RCOO]^-$ of the acyl chain at *m/z*227.0. While the relative intensity of the two peaks, $[M\text{-}H\text{-}RCOOH]^-/[M\text{-}H]^-$, is predominantly large for the ions 1a (lyso/14:0-PA), it is observed as the ratio is reversed for the CID spectra of ions 1b (14:0/lyso-PA) in Fig. 4b. Figure 4c shows CID spectra of molecular ions 2a (lyso/14:0-PG, *m/z*455.1) represented with diagnostic ions at *m/z*152.7 and 227.2, of which the former ions are generated from the dissociation of carboxylic acid from the parent ion that lost its glycerol head group ($-CHCHOHCH_2OH$, 74 Da), $[M\text{-}H\text{-}74\text{-}RCOOH]^-$, and the latter ions from the carboxylate anion $[C_{13}H_{27}COO]^-$. The intensity of $[M\text{-}H\text{-}74\text{-}RCOOH]^-$ ions is always larger for the sn-1 lyso-PG isomer than that of $[C_{13}H_{27}COO]^-$ ions, whereas the opposite phenomenon is observed for the sn-2 lyso-PG isomer, as shown in Fig. 4d. An $[M\text{-}H\text{-}74]^-$ peak appears with relatively weak intensities for both regioisomers. CID spectra shown in Fig. 5a are obtained from the dissociation of the molecular ions 3a, lyso/18:0-PS (*m/z*=524.0), resulting in two distinct fragment ions that are observed at *m/z*436.7, $[M\text{-}H\text{-}87]^-$, as parent ions after the loss of serine head groups ($C_3H_5NO_2$, 87 Da) and at *m/z* 153.0 as $[M\text{-}H\text{-}87\text{-}RCOOH]^-$ with the former ions prominent to the latter ones. In the inset of Fig. 5a, two minor peaks are shown and are identified as $[M\text{-}H\text{-}87\text{-}R'CH{=}C{=}O]^-$ at *m/z*171.3 and $[M\text{-}H\text{-}RCOOH]^-$ at *m/z*240.6, but these ion patterns fail to appear in the CID spectra of 18:0/lyso-PS in Fig. 5b. For LPS, typical carboxylate anion peaks are not observed regardless of the variation of CID energy from 30% to 55%. The same phenomenon is observed for the sn-2 isomers in Fig. 5b, and the fragment ion spectrum of the sn-2 regioisomers in Fig. 5b shows a similar pattern observed for the peak 3a. In this case, retention time is the only measure that distinguishes the regioisomers. LPI exhibits clear fragmentation patterns as shown in Fig. 5c, which is obtained from the molecular ions 4a, lyso/18:1-PI (*m/z*=597.4). Ions at *m/z*=434.4 and 415.6 are assigned as the fragment ions from the parent ions without the inositol head group ($C_6O_5H_{11}$, 162 Da) before and after the additional loss of water molecules, respectively. Fragmentation of the acyl chain leads to the formation of all three fragment ions of $[RCOO]^-$ at *m/z* 280.9, $[M\text{-}H\text{-}RCOOH]^-$ at *m/z*314.0, and $[M\text{-}H\text{-}R'CH{=}C{=}O]^-$ at *m/z*333.2. Among these ions, the intensity ratio of $[M\text{-}H\text{-}RCOOH]^-/[M\text{-}H\text{-}162\text{-}H_2O]^-$ is recognized as the diagnostic feature that distinguishes sn-1 from sn-2 regioisomers in which the intensity difference of these ions for 18:1/lyso-PI is reversed in such a way that $[M\text{-}H\text{-}162\text{-}H_2O]^-$ is observed as the base peak in Fig. 5d. CID spectra of PA, PS, and PI are not included in this paper since similar data can be found from the earlier works [25,27].

LOD values at the negative ion mode were calculated as 0.73 fmol (S=2.00, r^2=0.999) for 18:0-LPS, 0.89 fmol (S=0.47, r^2=0.999) for 14:0-LPA, and 1.1 fmol (S=0.50, r^2=0.988) for 12:0/12:0-PC at a signal-to-noise ratio of 3.

Profiling of LPLs and PLs in human plasma

The established run conditions for both positive and negative ion modes of nLC-ESI-MS/MS were applied to the plasma lipid extract sample, and their BPCs obtained at each run condition (used in Figs. 1 and 3) are shown in Fig. 6. Identified LPLs and PLs along with isomeric identification are listed in Table 1. In positive ion mode, 12 LPCs (six pairs of regioisomers), 14 LPEs (six pairs of regioisomers), 19 PCs, and 11 PEs were identified. For both groups of LPCs and LPEs, the same six pairs of regioisomers were found for acyl chain types such as 16:0, 18:0, 18:1, 18:2, 20:4, and 22:6, except that the acyl chain of 20:3 was additionally found for LPE. The common six acyl chains in both LPCs and LPEs are the same type of acyl chains reported for six LPA series of mouse plasma samples based on ESI-MS/MS analysis [6].

In the negative ion mode of analysis, the identified species included 18 LPAs, 4 LPGs, 2 LPSs, 5 PAs, 8 PGs, 3 PSs, and 16 PIs and are listed in Table 1. LPA molecular types identified in the negative ion mode of the nLC-ESI-MS/MS run were diverse compared to the other LPGs and

LPSs, and the LPI molecule was not found in this run. Types of LPA molecules found in the human plasma in Table 1 were nine pairs (14:0, 16:0, 16:1, 16:2, 18:0, 18:2, 18:3, 20:4, 22:6) including five out of six acyl chain types found in LPCs listed in Table 1 except the acyl chain 18:1. The LPA list also includes the six out of seven acyl chain types found in LPEs except for the acyl chain 20:3. This is because LPA molecules in human blood are known to generate from LPCs and LPEs by the enzyme lysophospholipase D [5, 33].

Conclusions

This study demonstrates that nLC-ESI-MS/MS analysis of human plasma in both positive and negative ion modes provides a simultaneous separation of LPLs and PLs along with complete structural analysis with a data-dependent CID experiment. Identified LPLs and PLs from the human plasma sample included 50 LPLs and 62 PLs in total using a reversed phase capillary LC column. While the current study demonstrates qualitative profiling of LPLs and PLs from a human plasma sample, the technique can be applied to quantitative analysis to determine the relative differences in composition and concentration of LPLs and PLs. Since LPAs and LPCs are known to be potential biomarkers of ovarian cancer [8] and colorectal cancer [9], respectively, the current method can be utilized for high-speed quantitative nLC-ESI-MS analysis in clinical studies by adjusting the LC gradient run condition to scan only LPA or LPC species that are preliminarily identified via data-dependent CID analysis.

Acknowledgements This study was supported by a grant (NRF-2010-0014046) from the National Research Foundation of Korea.

References

1. Brouwers JFHM, Vernooji EAAM, Tielens AGM, van Golde LMG (1999) J Lipid Res 40:164–169
2. Wright MM, Howe AG, Zaremberg V (2004) Biochem Cell Biol 82:18–26
3. Wolf C, Quinn PJ (2008) Lipid Res 47:15–36
4. Barroso B, Bischoff R (2005) J Chromatogr B 814:21–28
5. Ishida M, Imagawa M, Shimizu T, Taguchi R (2005) J Mass Spectrom Soc Jpn 53:217–226
6. Zhao Z, Xu Y (2009) J Chromatogr B 877:3739–3742
7. Xu Y, Shen Z, Wiper DW, Wu M, Morton RE, Elson P, Kennedy AW, Belinson J, Markman M, Casey G (1998) JAMA 280:719–723
8. Sutphen R, Xu Y, Wilbanks GD, Fiorica J, Grendys EC, LaPolla JPJ, Arango H, Hoffman MS, Martino M, Wakeley K, Griffin D, Blanco RW, Cantor AB, Xiao YJ, Krischer JP (2004) Cancer Epidemiol Biomark Prev 13:1185–1191
9. Zhao Z, Xiao Y, Elson P, Tan H, Plummer SJ, Berk M, Aung PP, Lavery IC, Achkar JP, Li L, Casey G, Xu Y (2007) J Clin Oncol 25:2696–2701
10. Hu C, Heijden R, Wang M, Greef J, Hankemeier T, Xu G (2009) J Chromatogr B 877:2836–2846
11. Kuksis A, Myher JJ, Marai L (1984) J Am Oil Chem Soc 61:1582–1589
12. Heller DN, Murphy CM, Cotter RJ, Fenselau C, Uy OM (1988) Anal Chem 60:2787–2791
13. Fuchs B, Schiller J, Süβ R, Schürenburg M, Suckau D (2007) Anal Bioanal Chem 389:827–834
14. Rohlfing A, Muthing J, Pojlentz G, Distler I, Peter-Katalinc J, Berkenkamp S, Dreisewerd K (2007) Anal Chem 79:5793–5808
15. Helmy F, Rothenbacher F, Nosavanh L, Lowery J, Juracka A (2007) J Planar Chromatogr Mod TLC 20:209–215
16. Hsu F-F, Turk J (2003) J Am Soc Mass Spectrom 14:352–363
17. Hsu F-F, Turk J (2009) J Chromatogr B 877:2673–2695
18. Han X, Gross RW (1996) J Am Chem Soc 118:451–457
19. Khaselev N, Murphy RC (2000) J Am Soc Mass Spectrom 11:283–291
20. Wang H-Y, Liu C, Wu H-W, Kuo J (2010) Rapid Commun Mass Spectrom 24:2057–2064
21. Taguchi R, Houjou T, Nakanishi H, Yamazaki T, Ishida M, Imagawa M, Shimizu T (2005) J Chromatogr B 823:26–36
22. Bang DY, Kang D, Moon MH (2006) J Chromatogr A 1104:222–229
23. Bang DY, Ahn E, Moon MH (2007) J Chromatogr B 852:268–277
24. Wang C, Xie S, Yang J, Yang Q, Xu G (2004) Anal Chim Acta 525:1–10
25. Kim H, Ahn E, Moon MH (2008) Analyst 133:1656–1663
26. Kim H, Min HK, Kong G, Moon MH (2009) Anal Bioanal Chem 393:1649–1656
27. Min HK, Kong G, Moon MH (2010) Anal Bioanal Chem 396:1273–1280
28. Yoon H-R, Kim H, Cho S-H (2003) J Chromatogr B 788:85–92
29. Murph M, Tanaka T, Pang J, Felix E, Liu S, Trost R, Newman AR, Mills G (2007) Methods in enzymology, ch. 1, vol 433. Elsevier, Amsterdam
30. Scherer M, Schmitz G, Liebisch G (2009) Clin Chem 55:1218–1222
31. Fang N, Yu S, Badger TM (2003) J Agric Food Chem 51:6676–6682
32. Folch J, Lee M, Stanley GHS (1957) J Biol Chem 226:497–509
33. Tokumura A, Majima E, Kariya Y, Tominaga K, Kogure K, Yasuda K, Fukuzawa K (2002) J Biol Chem 277:39436–39442